

A Frequency Selective Radome With Wideband Absorbing Properties

Filippo Costa, *Member, IEEE*, and Agostino Monorchio, *Fellow, IEEE*

Abstract—A frequency selective radome is presented, acting as a pass band filter at a given frequency band, while behaving as an absorber above the transmission band. The pass band behavior is obtained by a metallic FSS realized through a compact interdigitated Jerusalem cross element characterized by a very large rejection band. The metallic FSS is used as the ground plane of a thin wideband absorber based on resistive high-impedance surfaces within the total reflection band. The outer absorber reduces the signature of the antenna system when the radome is illuminated by out of band signals. The resistive FSS which comprises the absorber is designed so to minimize losses within the transmitting band of the radome. The composite structure is thoroughly analyzed by an efficient equivalent circuit approach and by full-wave numerical simulations.

Index Terms—Electromagnetic absorbers, high-impedance surfaces (HIS), low RCS, metamaterials, radar absorbing material (RAM), radome, resistive frequency selective surfaces (RFSS).

I. INTRODUCTION

A radome is a cover placed over the antenna that protects the radiating element from its physical environment (e.g., wind, rain, ice, sand, and ultraviolet rays). It protects the antenna's exposed parts with a sturdy, weatherproof material, typically fiberglass, which keeps debris or ice away from the antenna to prevent any serious damage or malfunctioning. From an electromagnetic point of view, a radome should be transparent to radio frequencies so that it does not degrade the electrical performance of the enclosed antenna.

Under many circumstances, it is desirable to employ a frequency selective radome in order to prevent coupling from nearby transmitting antennas that may interfere with the electronic circuitry [1]. Other than the control on out of band emissions, the role of the radome can be of crucial importance in reducing the antenna Radar Cross Section (RCS) [2], [3]. To this purpose, a radome is usually designed as a frequency selective filter which allows the operating frequencies to pass with the least amount of insertion loss, whereas it reflects the out of band signals [4]–[6]. Generally, in-band RCS is dominated by the antenna itself, not by the radome, whereas

far out of band, the RCS will be dominated by the shape and by the reflection properties of the radome [7]. Consequently, the frequency selectivity together with a proper shape of the radome tends to reduce the antenna RCS since impinging out of band power, representing a potential interrogation signal of an unknown radar, would be reflected towards a specular direction with a minimum monostatic reflection. This approach can be classified as a fictitious RCS reduction technique since it is effective only for monostatic interrogations (no benefits against bistatic or passive radar) and if no additional scatterers are located in the close proximity of the antenna [8].

More in general, an ideal low-RCS radome should transmit the in-band power and absorb the incoming out of band power. This solution is usually not considered since it is a common belief that the employment of lossy material for manufacturing a radome causes a high insertion loss. To the best of our knowledge, the sole attempt to design a transmissive and absorbing radome has been presented in [9], where only the qualitative working principle of the structure is illustrated. The authors of the patent present a multilayer structure formed by a frequency selective surface and by the artificial absorbing coating described in [10] which is composed by a uniform layer of conductive fibers. The patent does not present any quantitative result (neither insertion loss nor absorptive properties) but it is well known that the use of a uniform resistive layer on top of a frequency selective structure spoils the transmissivity of the radome [11], [12] making the proposed design impractical.

The aim of this paper is to synthesize a transmissive/absorbing radome by means of opportunely designed resistive and metallic periodic surfaces in order to achieve high in-band transmission and, at the same time, a wideband absorption behavior. The main goals to achieve are summarized below:

- Low in-band insertion loss both for transmitted and received signals.
- Wideband absorption of out of band incoming signals.
- Periodicity of the frequency selective surface lower than a wavelength at the upper frequency limit of the absorption band for avoiding grating lobes.

The paper is organized as follows: in the next Section, a description of the novel structure under analysis is presented. The main components of the radome are summarized and a useful equivalent circuit of the structure is presented; in Section III the design of a pass-band FSS filter with a large rejection band is addressed. Section IV deals with the choice of a resistive FSS composing the absorptive side of the radome which minimizes the insertion loss. In Section V the numerical results obtained with the final design of the radome are shown and validated by two independent full-wave commercial codes.

Manuscript received December 22, 2010; revised November 04, 2011; accepted November 24, 2011. Date of publication April 12, 2012; date of current version May 29, 2012.

The authors are with Department of Information Engineering, University of Pisa, 56122 Pisa, Italy and also with RaSS National Laboratory, CNIT, Pisa, Italy (e-mail: filippo.costa@iet.unipi.it; a.monorchio@iet.unipi.it).

Color versions of one or more of the figures in this paper are available online at <http://ieeexplore.ieee.org>.

Digital Object Identifier 10.1109/TAP.2012.2194640

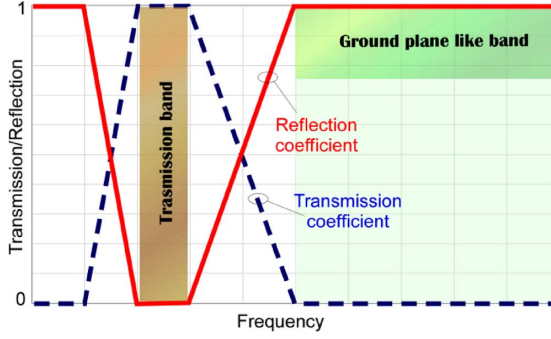


Fig. 1. Ideal transmission and reflection coefficient of the metallic FSS filter.

II. DESCRIPTION OF THE STRUCTURE

In order to transform an antenna into a low-RCS structure, the radome cover should be absorbent when illuminated by out of band signals. Considering the impossibility of employing a real ground plane, one might consider to exploit a metamaterial absorber design not requiring the presence of a ground plane. Unfortunately, such kind of structures are inherently narrow band [13]. A wideband absorption profile can be obtained only by placing one or more lossy surfaces on top of a ground plane [14]. We propose a design based on a pass-band metallic frequency selective filter characterized by a wide reflection band so that the FSS can be also used as a ground plane for an external absorbing structure. The ideal transmission/reflection profile of the metallic FSS filter is represented in Fig. 1. The thin wideband absorbing structure is synthesized by placing an additional resistive frequency selective surface on top of a foam spacer glued on the metallic FSS. Within the frequency range where the FSS behaves as a ground plane, the multilayer absorbs impinging signals as a wideband high-impedance surface absorber [15], [16]. A three dimensional representation of the proposed structure is shown in Fig. 2.

In order to obtain low insertion loss of the composite structure within the operating band of the antenna, the resistive FSS has to be almost transparent in this band.

Since the operating bands of absorbing and transmissive parts of the radome are significantly separated in the spectrum, it is expected that the periodicity of the metallic FSS and the resistive one are dissimilar. This aspect leads to the following drawbacks: Firstly, the periodicity of the metallic FSS cannot exceed one wavelength at the maximum operating frequency of the absorber for avoiding the presence of the grating lobes within the absorber working band. Additionally, a full-wave analysis of cascaded frequency selective surfaces with dissimilar repetition periods can be accomplished only if the periodicities of the FSSs are commensurate, i.e. the ratio of the periods is a rational number. However, this design procedure leads to the analysis of several unit cells of the cascaded FSS screens requiring time consuming simulations. For this reason, at the first stage of the design process, an approximate analysis is performed by a simple equivalent transmission line of the structure. The equivalent circuit analysis allows also achieving insight into the physics of the electromagnetic device.

The equivalent network of the investigated structure is shown in Fig. 3.

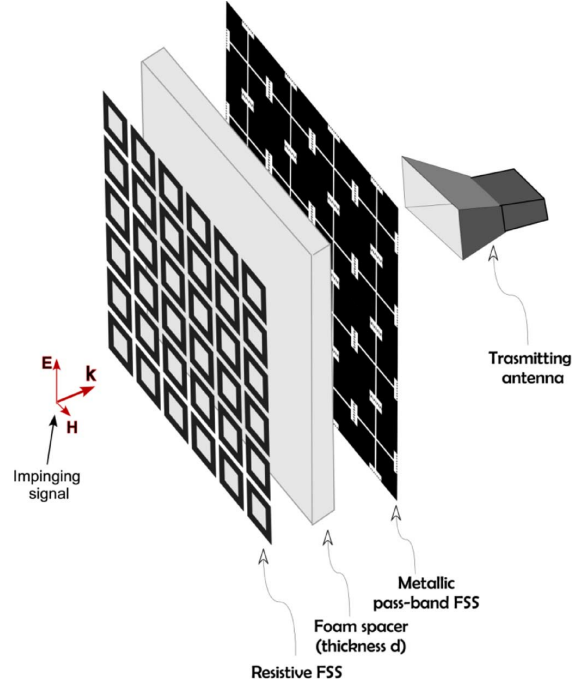


Fig. 2. 3D sketch of the absorbing/transmissive radome.

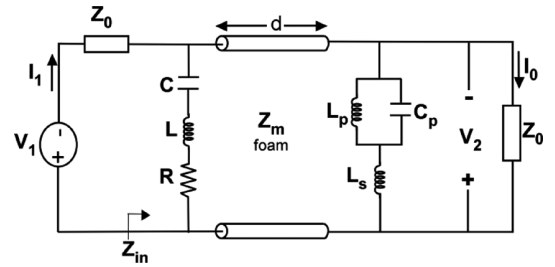


Fig. 3. Transmission line equivalent of the transmissive/absorbing radome.

In the circuit analysis, a metallic pass-band FSS can be simply represented by a parallel LC circuit if the filter is realized with a simple FSS unit cell such as a cross or a square loop. If the unitary cell of the FSS is a Jerusalem cross, a series inductance L_s other than the parallel LC is needed [17]. The capacitive resistive FSS is instead approximated by a series RLC circuit [16]. The reflection coefficient of the composite structure is obtained for both normal and oblique incidence by computing the input impedance of the circuit reported in Fig. 3 according to classical transmission line rules. The impedance across the dielectric slab is computed as follows:

$$Z_v^{TE,TM} = Z_m^{TE,TM} \frac{[Z_L^{TE,TM} + Z_m^{TE,TM} \tanh(i\beta_m d)]}{[Z_m^{TE,TM} + Z_L^{TE,TM} \tanh(i\beta_m d)]} \quad (1)$$

where Z_L is the load impedance. Z_m, β_m, k_m are:

$$Z_{mTE} = \frac{\omega\mu_0}{\beta_m}, \quad Z_{mTM} = \frac{\beta_m}{\omega\epsilon_0\epsilon_r}$$

$$\beta_m = \sqrt{k_m^2 - k_t^2}, \quad k_t = k_0 \sin(\theta), \quad k_m = k_0 \sqrt{\epsilon_r \mu_r} \quad (2)$$

where θ is the incident angle k_0 is the free space propagation constant and k_t is the transverse wavevector. Once the input impedance of the structure is derived, the reflection coefficient is obtained according to the following relation:

$$\Gamma_{receiv} = \frac{Z_{in}^{TE,TM} - Z_0^{TE,TM}}{Z_{in}^{TE,TM} + Z_0^{TE,TM}} \quad (3)$$

where Z_{in} is the input impedance of the composite structure Z_0^{TE} is $\zeta_0 / \cos(\theta)$ and Z_0^{TM} is $\zeta_0 \cdot \cos(\theta)$, being ζ_0 the free space impedance. The reflection coefficient of the analyzed network coincides with the S_{11} since the load is represented by the free space impedance. The transmission coefficient of the radome (S_{21}) is evaluated as follows [18]:

$$T_{receiv} = S_{21_receiv} = \frac{2V_2}{V_1} \left| \frac{2Z_0^{TE,TM}}{C(Z_0^{TE,TM})^2 + DZ_0^{TE,TM} + AZ_0^{TE,TM} + B} \right| \quad (4)$$

V_1 and V_2 represent the voltages at the input and at the output of the system and the terms A, B, C, D are the elements of the transmission line matrix of the entire system which is evaluated as the product of the three cascaded matrices [19]:

$$\begin{bmatrix} A & B \\ C & D \end{bmatrix} = \begin{bmatrix} 1 & 0 \\ \frac{1}{Z_{FSS}^{res}} & 1 \end{bmatrix} \begin{bmatrix} \cos(\beta_m d) j Z_m \sin(\beta_m d) \\ j \frac{\sin(\beta_m d)}{Z_m} \cos(\beta_m d) \end{bmatrix} \times \begin{bmatrix} 1 & 0 \\ \frac{1}{Z_{FSS}^{metal}} & 1 \end{bmatrix} \quad (6)$$

where Z_{FSS}^{res} and Z_{FSS}^{metal} are the approximate impedances of the resistive and the metallic FSS, respectively. The inductances and the capacitances of the employed FSSs are computed by matching the normal incidence full-wave response of the elements in freestanding configuration. A detailed description of the procedure is available in [17]. The energy absorbed by the structure is obtained by applying the following relation:

$$A_p^{dB} = -10 \cdot \log_{10} (T_{receiv}^2 + \Gamma_{receiv}^2). \quad (7)$$

In order to present a practical design of the structure, a realistic operating frequency of the antenna has been chosen. It is assumed that the antenna operates within the C band and in particular between 4.2 GHz and 4.9 GHz. Consequently, the electromagnetic absorber operates beyond the upper frequency limit of the antenna working band.

III. DESIGN OF THE PASS-BAND FSS WITH A LARGE REJECTION BAND AND SMALL PERIODICITY

The simplest FSS element acting as a pass-band filter is an inductive cross. The use of an inductive square loop is discarded since it is not a simply connected shape (it is composed by two unconnected metallic parts) and consequently not easily manufacturable if the FSS filter is realized with thick metal for power handling purposes [14], [19]. In Fig. 4 the reflection and

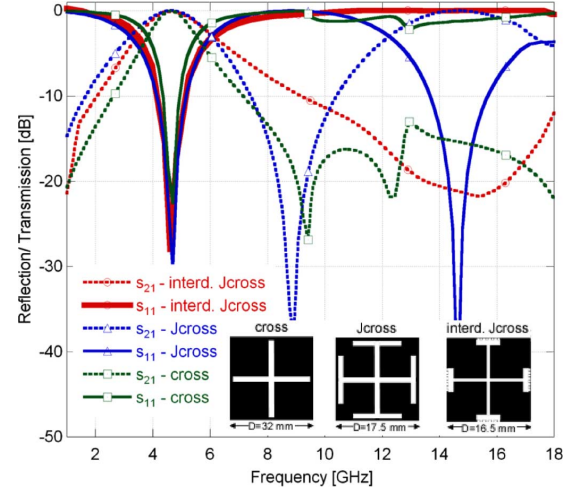


Fig. 4. Reflection and transmission coefficient of three different pass-band FSS elements. The periodicity of the cross element leads to the onset of grating lobes at 9.3 GHz.


transmission coefficients of three different pass-band FSS filters based on the cross element are reported. The simple cross allows the realization of a pass-band filter operating in C-band with a FSS cell periodicity larger than 30 mm. Such large repetition period causes the onset of grating lobes right above 10 GHz. This aspect makes the simple cross element not suitable for designing a filter with a wideband unitary reflecting behavior. In order to reduce the period of the FSS filter, a Jerusalem cross element is selected. In this case, a smaller periodicity (i.e. 17.5 mm) allows obtaining the pass-band behavior in the desired frequency band. However, the frequency response of the Jerusalem cross FSS is characterized by a second pass-band resonance at 15 GHz, that is, the FSS acts as a ground plane only between 8 GHz and 11 GHz. In order to enlarge the unitary reflection bandwidth of the filter and reduce at the same time the periodicity, an interdigitated Jerusalem cross element has been designed. In this case the pass-band behavior is obtained at 4.6 GHz with a periodicity of 16.5 mm and the total reflection band extends from 8 GHz to 18 GHz.

IV. RESISTIVE HIGH-IMPEDANCE SURFACE ABSORBER WITH A LOW INSERTION LOSS WITHIN THE ANTENNA OPERATING BAND

According to the previous finding, the designed inductive filter can be employed as ground plane of the outer absorber from 8 GHz to 18 GHz. On the other hand, the absorbing structure has to fulfill an essential requirement: it has to be transparent in the working band of the antenna. To aim a low profile wideband radar absorber based on resistive frequency selective surfaces is employed [16]. The wideband absorber is formed by a suitably designed square loop shaped resistive FSS on top of a thin grounded dielectric substrate. The thickness of such absorbing structure allows approaching the physical limitation for non-magnetic Radar Absorbing Materials (RAM) [21].

With the aim of verifying the transparency of the absorber within the working band of the antenna, the transmission profile of the freestanding FSS composing the absorber is initially analyzed. Let us consider three different capacitive square loop

TABLE I
PHYSICAL AND EQUIVALENT PARAMETERS OF THE RESISTIVE FSS

Resistive narrow square loop FSS			
	Actual parameters		
	D [mm]	Surface Res. [Ω/sq]	
	11	15	
	Lumped parameters		
	L [nH]	C [pF]	R [Ω]
	4.1	0.024	260

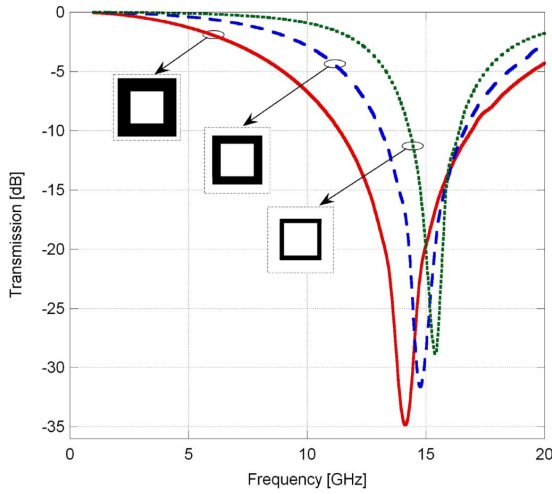


Fig. 5. Transmission coefficient of three different square loop shaped metallic FSSs. The periodicity of the FSS is equal to 11 mm in all cases.

FSSs with the free space resonance located around 15 GHz as required for designing the wideband absorber [16]. All the elements are characterized by the same periodicity D , i.e. 11 mm. The side lengths of the loops, from the narrowest to the widest one, are $10/16D$, $12/16D$ and $14/16D$ while the thicknesses of the loop are $1/16D$, $2/16D$ and $3/16D$, respectively. The geometrical dimensions of two of the three analyzed elements are reported in Table I and Table III shown in the next section. In Fig. 5 the transmission profile of the three square loops is reported. The FSSs are initially analyzed without considering the resistive losses. The wide printed square loop used in [16] is characterized by a high insertion loss at 4.6 GHz but, as the loop becomes narrower, the insertion loss is remarkably lowered down to 0.1 dB. Anyway, it is clear that the frequency selective surface cannot be metallic for obtaining absorption and the insertion loss of the filter has to be verified in the case of resistive FSSs. In Fig. 6 the transmission coefficient of the narrowest square loop FSS is reported for different values of surface resistance. As it is apparent in the inset of the figure, the insertion loss in the operating band of the antenna does not exceed 0.7 dB even for high values of surface resistance. In order to realize a wideband absorber with a spacer thickness of 5 mm, it is necessary, as remarked in [16], to synthesize an equivalent series lumped resistance of roughly 260 Ω . Such lumped value leads to different distributed surface resistances depending on the filling factor of the FSS element [16]. If the printed percentage of the unit cell is low as in the case of the narrow square loop, a surface resistance of 10–15 Ω/sq is sufficient.

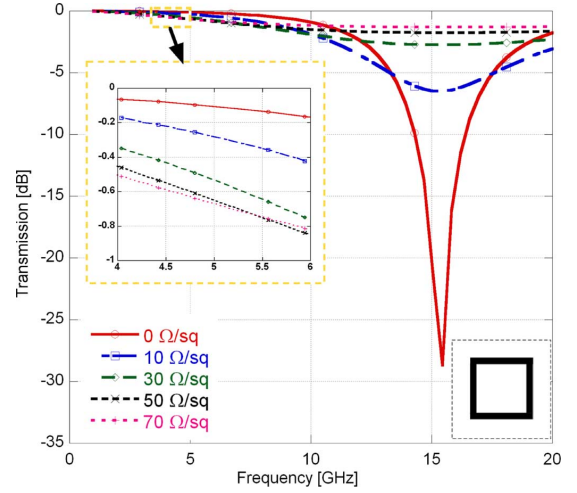


Fig. 6. Transmission coefficient of the thin square loop shaped FSS with different values of the surface resistance. In the inset it is highlighted the transmission coefficient of the FSS within the operating band of the antenna.

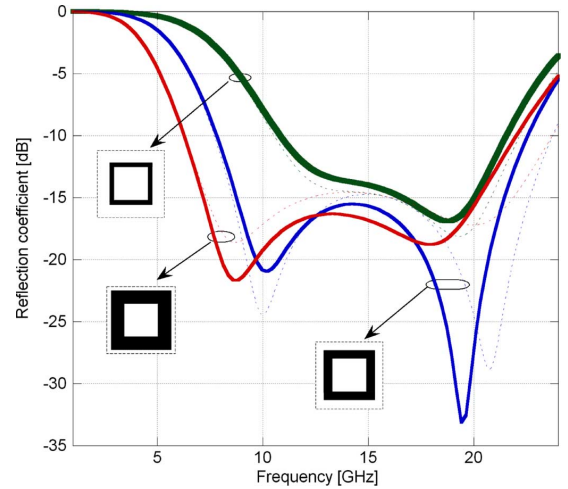


Fig. 7. Reflection coefficient of the absorbing structure with metallic ground. The thickness of the absorber is 5 mm in all cases.

In Fig. 9, the performance of a 5 mm thick wideband absorber with metallic ground plane are analyzed for the three different FSS elements. The design proposed in [16] is the most wideband but, as remarked above, it gives rise to high losses within the antenna working band. The narrowest square loop can be classified as the best compromise if the insertion loss is considered, as it is common practice in a radome design, the key parameter. Even if the absorption bandwidth is reduced with respect to the optimal absorber design, it is still satisfying. The intermediate wide square loop can be employed if a slightly higher in-band loss is acceptable.

V. PERFORMANCE OF THE RADOME

In this section the performance of the multilayer radome are analyzed both when the antenna is in transmitting and in receiving mode. The transmitting mode is analyzed considering a plane wave impinging on the metallic side of the radome, while

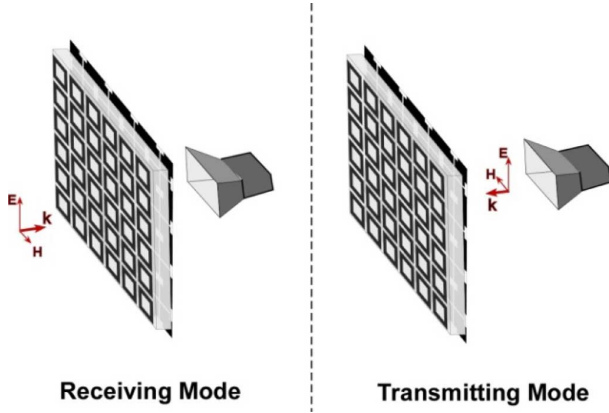


Fig. 8. A 3D sketch representing the receiving and transmitting modes.

TABLE II
PHYSICAL AND EQUIVALENT PARAMETERS OF THE PASS-BAND FSS

Interdig. Jerusalem cross FSS			
Actual parameters [mm]			
L		p	w
13.95		4.65	0.46
m	m_1	s	g
0.82	0.23	0.35	0.93
Lumped parameters			
L_p [nH]		C_p [pF]	L_s [nH]
3.74		0.313	0.372

the receiving mode is analyzed by exciting a plane wave towards the absorbing side (see Fig. 8).

The structure is analyzed with periodic boundary conditions by two independent full-wave codes (i.e. HFSS v.11 and CST Microwave Studio 2011). For achieving a unit cell with the same macro-period, 4 unit cells of the metallic screen and 9 resistive square loop unit cells have been cascaded obtaining macro-cells with a periodicity of 33 mm. The full-wave simulations are very time consuming (around 50 hours) since the metallic pass-band FSS is interdigitated and the periodicities of the filters are dissimilar. For this reason the use of the equivalent circuit approach results of great practical usefulness. The results obtained with the narrowest square loop are initially reported. The geometrical and electrical parameters of the composite structure are reported in Table I and in Table II.

A. Normal Incidence

In Fig. 9 the reflection and transmission coefficients of the radome in the transmitting mode are shown. The insertion loss at 4.6 GHz is close to the 0.3 dB which can be considered an excellent result considering that the electromagnetic field crosses a resistive FSS. The reflection and transmission coefficients, similarly to a metallic radome, preserve a frequency selectivity behavior which is beneficial for avoiding spurious radiation towards nearby electronic circuitry.

In Fig. 10 the transmission and the reflection coefficients of the radome illuminated by a normal incident plane wave from the absorbing side are reported. The transmission coefficient of the structure, as it occurs for every passive device [18], is exactly equivalent to the one found in the transmitting mode.

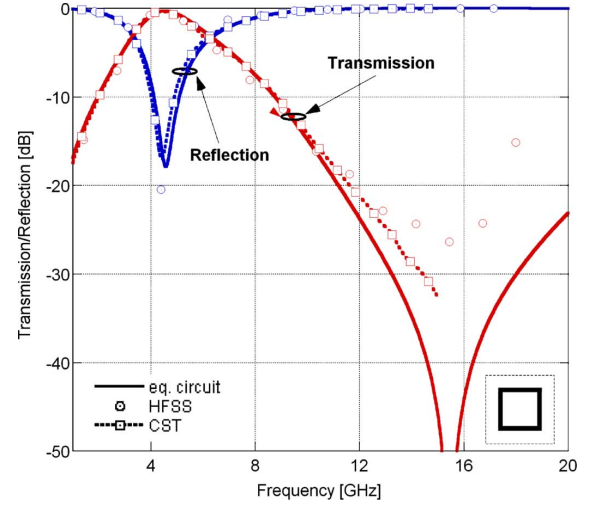


Fig. 9. Transmission and reflection coefficient of the radome in transmitting mode.

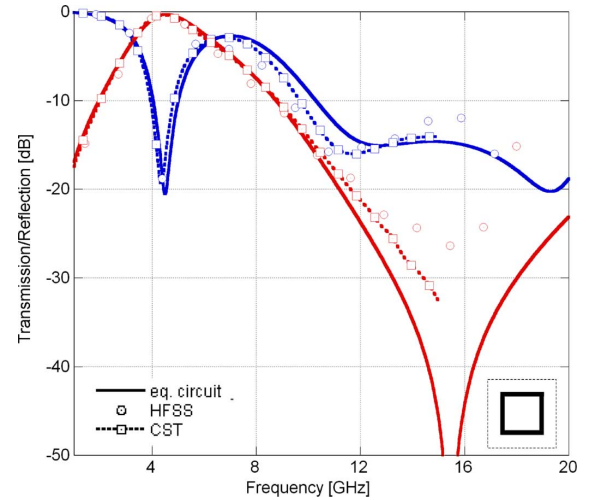


Fig. 10. Transmission and reflection coefficient when the radome is illuminated by a normal incident plane wave (receiving mode).

This allows the antenna to receive and transmit simultaneously within its working frequency band. The reflection coefficient of the composite structure in the receiving mode is instead undoubtedly different from the one obtained in the transmitting mode since the reflected signal is lowered by the presence of the absorber. Since low reflection does not repeatedly imply high absorption, the amount of absorbed power is reported in Fig. 11. By observing the curve, it is apparent that the structure drastically reduces the reflected power from 10 GHz to 18 GHz and it introduces only few fractions of dB of losses within the antenna frequency band. The results obtained by the equivalent circuit approach are compared against the ones obtained by full-wave simulations in order to verify the accuracy of such fast analysis. The simulations with CST are available only up to 15 GHz since the computation burden at higher frequencies becomes too heavy.

The radome performs absorption only above the working band of the antenna while, within the low frequency range, it reflects signals without absorption. This is basically due to the

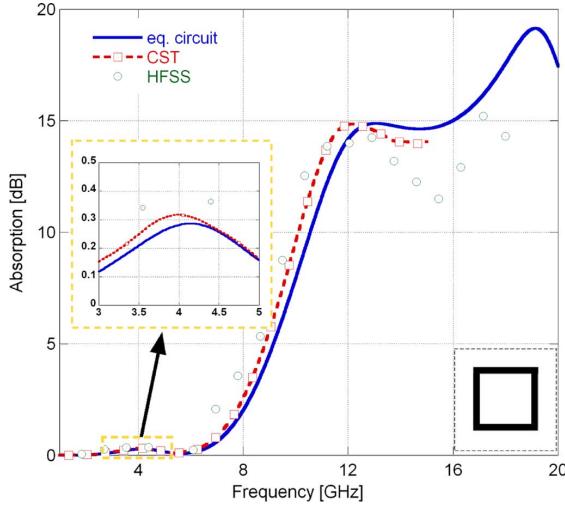


Fig. 11. Energy absorbed by the radome when it is illuminated by a normal incident plane wave (receiving mode).

low distance between the FSSs (only 5 mm) which allows to perform absorption only in the upper frequency range. In order to perform absorption across an octave in the lower frequency band (i.e. 1–2 GHz for instance) a thicker structure (roughly 40 mm) and larger FSS periodicity (roughly 88 mm) would be required. In this case, the absorption at the higher frequency band should be re-evaluated and the presence of grating lobes should be taken into account.

B. Oblique Incidence

One of the main requirements for a practical radome is the preservation of the transmissive properties as a function of the incident angle. In Fig. 12 and in Fig. 13 the reflection and transmission coefficient of the radome in receiving mode are shown for a 30° oblique incident wave. The pass-band stability of the proposed structure as a function of the incident angle is excellent since a cross element with long and very thin arms is typically an angular stable FSS element [17]. The absorption properties, as expected, degrade as a function of the incident angle [16]. In addition, the choice of the inductive FSS periodicity equal to 16.5 mm fixes the frequency at which the first grating lobe appears at 18.2 GHz at normal incidence. As a consequence, some spikes are observed below 18 GHz at oblique incident angles. In our case, according to the theory [14], the first grating lobe appears at 12.12 GHz at 30° and 9.77 GHz at 45° and so on. With the presence of grating lobes, the computed reflection coefficient is still valid for specular reflection but it cannot be excluded that some energy is reflected in other directions too. In order to avoid this undesired phenomenon, the unit cell of the pass band FSS should be even more miniaturized while preserving the same transmissive/reflective properties shown in Fig. 4.

To this aim, the final end loading segment of the Jerusalem cross, with length p , could be lengthen in order to enhance the capacitive coupling. The occurrence of grating lobes leads to the presence of spurious peaks in full-wave computations but it is worth to underline that the full-wave results follow on average the curves obtained by using the equivalent circuit approach. The transmission line analysis is valid also for oblique

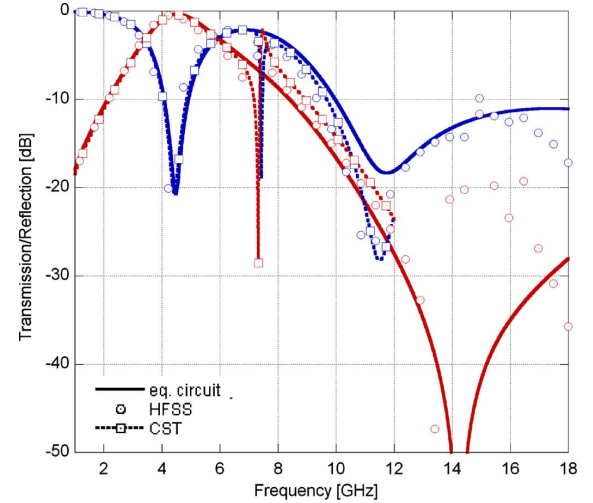


Fig. 12. Transmission and reflection coefficient in receiving mode at oblique incidence. Incident angle: 30 degree; polarization: TE.

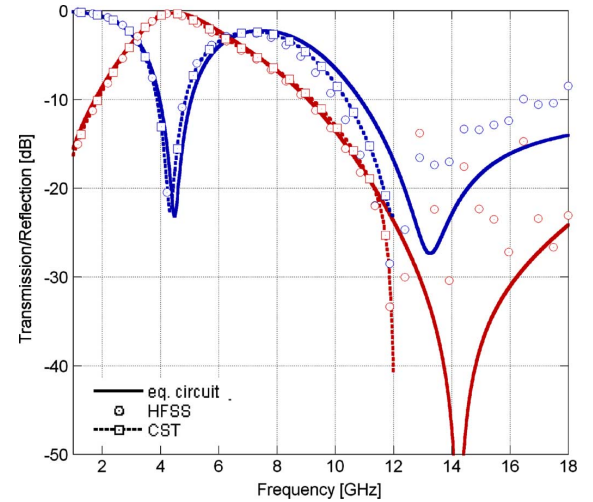


Fig. 13. Transmission and reflection coefficient in receiving mode at oblique incidence. Incident angle: 30 degree; polarization: TM.

incident waves but it neglects higher order contributions due to the propagation of high order Floquet modes. Fig. 14 reports a comparison between the transmission coefficients of the radome obtained at normal incidence and for two oblique incident angles, i.e. 30° and 45°. As is well known, the bandwidth for TM polarization tends to increase as the incident angle grows up, while the resonance frequency shows a moderate shift towards lower frequencies [22]. The opposite trend is valid for TE polarization. The pass-band properties of the multilayer structure are satisfactorily stable both for TE and TM polarization.

C. Enlargement of the Absorption Band

If a slightly higher in-band insertion loss can be tolerated, the RCS reduction can be further improved by using a wider square loop FSS. In particular the following simulations show the results obtained with the intermediate wide square loop. The geometrical and the equivalent lumped parameters of the resistive FSS, together with a sketch of the FSS element, are summarized in Table III.

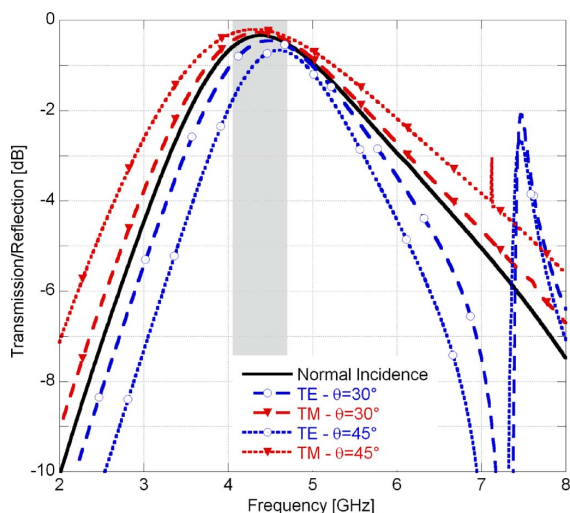
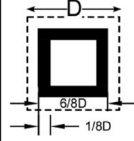


Fig. 14. Transmission coefficient of the radome for normal and oblique incidence obtained with CST Microwave Studio 2011.

TABLE III
PHYSICAL AND EQUIVALENT PARAMETERS OF THE INTERMEDIATE SQUARE LOOP RESISTIVE FSS

Resistive intermediate square loop FSS			
	Actual parameters		
	D [mm]	Surface Res. [Ω/sq]	
	11	40	
	Lumped parameters		
	L [nH]	C [pF]	R [Ω]
	2.475	0.0465	260

In Fig. 15 the transmission and reflection coefficients of the composite radome in receiving mode at normal incidence are shown. The results for the transmitting mode are omitted since the transmission coefficient is identical to the one obtained in receiving mode. By observing Fig. 15 it is evident that the absorption band is enlarged at the cost of a reduced transmissivity within the working band of the antenna. In Fig. 16 the energy absorbed by the structure in the receiving mode is shown.

As expected, a reduction of 15 dB of the reflected power is obtained immediately before 10 GHz up to 18 GHz. The in-band insertion loss increases up to 1.25 dB in this case.

VI. CONCLUSION

We have presented a novel design of a frequency selective radome which is able to absorb impinging electromagnetic signals above the operating band of the antenna. The radome is realized by a resistive frequency selective surface placed on top of a metallic FSS realized by an interdigitated Jerusalem cross element. The structure, unlike the usual low RCS radome design which totally reflects the incoming power out of the antenna operating band, provides a tangible reflectivity reduction without compromising the in-band performance. The insertion loss is minimized to 0.3 dB and the -15 dB absorption bandwidth spans from 10 GHz to 18 GHz. The analysis performed by an accurate equivalent circuit approach is verified by full-wave simulations obtained with two independent simulations codes.

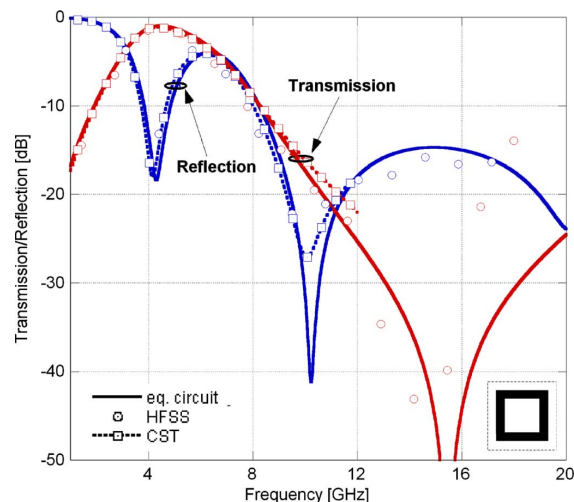


Fig. 15. Transmission and reflection coefficient when the radome is illuminated by a normal incident plane wave. The resistive FSS is composed by the intermediate wide square loop.

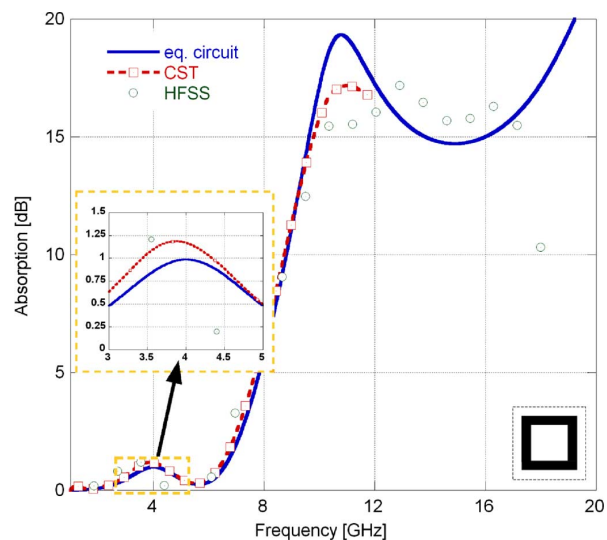


Fig. 16. Energy absorbed by the radome when it is illuminated by a normal incident plane wave. The resistive FSS is composed by the intermediate wide square loop with a surface resistance of $40 \Omega/\text{sq}$.

ACKNOWLEDGMENT

The authors acknowledge the support of CST for providing additional resources and technical assistance for the parallel version of CST Microwave Studio.

REFERENCES

- [1] D. J. Kozakoff, *Analysis of Radome-Enclosed Antennas*. Norwood, MA: Artech House, 1997.
- [2] J. D. Lynch, *Introduction to RF Stealth*. Raleigh, NC: SciTech Publishing, 2004.
- [3] D. Richardson, *Stealth Warplanes*. London, U.K.: Salamander Books, 2001.
- [4] E. Martini, F. Caminita, M. Nannetti, and S. Maci, "Fast analysis of FSS radome for antenna RCS reduction," in *Proc. IEEE Int. Symp. on Antennas and Propagation Society*, Jul. 2006, pp. 1801–1804.
- [5] P. C. Kim, D. G. Lee, I. S. Seo, and G. H. Kim, "Low-observable radomes composed of composite sandwich constructions and frequency selective surfaces," *Compos. Sci Technol*, vol. 68, no. 9, pp. 2163–2170, 2008.

- [6] H. Chen, X. Hou, and L. Deng, "Design of frequency—Selective surfaces radome for a planar slotted waveguide antenna," *IEEE Antennas Wireless Propag. Lett.*, vol. 8, pp. 1231–1233, 2009.
- [7] Y. C. Chang, "Low Radar Cross Section Radome," U.S. Patent 6,639,567 B2, Oct. 28, 2003.
- [8] J. A. Adam, "How to design an invisible aircraft," *IEEE Spectrum*, pp. 26–31, Apr. 1988.
- [9] W. S. Arceneaux, R. D. Akins, and W. B. May, "Absorptive/Transmissive Radome," U.S. Patent 5,400,043, May 21, 1995.
- [10] M. Stander, "Radar Absorptive Coating," U.S. Patent 3,599,210, Aug. 1971.
- [11] G. I. Kiani, A. R. Weily, and K. P. Esselle, "A novel absorb/transmit FSS for secure indoor wireless networks with reduced multipath fading," *IEEE Microwave Wireless Compon. Lett.*, vol. 16, no. 6, pp. 378–380, June 2006.
- [12] A. Motevasselian and B. L. G. Jonsson, "Partially transparent Jaumann like absorber applied to a curved structure," *Hindawi Int. J. Antennas Propag.*, vol. 2011.
- [13] F. Bilotti and L. Vegni, "Design of metamaterial-based resonant microwave absorbers with reduced thickness and absence of a metallic backing," *Metamaterials and Plasmonics: Fundamentals, Modelling, Applications* S. Zouhdi, A. Sihvola, and A. P. Vinogradov, Eds., ser. NATO Science for Peace and Security Series B, 2009, pp. 165–174.
- [14] A. Kazemzadeh, "Nonmagnetic ultrawideband absorber with optimal thickness," *IEEE Trans. Antennas Propag.*, vol. 59, no. 1, pp. 135–140, Jan. 2011.
- [15] B. A. Munk, *Frequency Selective Surfaces—Theory and Design*. New York: Wiley, 2000.
- [16] F. Costa, A. Monorchio, and G. Manara, "Analysis and design of ultra thin electromagnetic absorbers comprising resistively loaded high impedance surfaces," *IEEE Trans. Antennas Propag.*, vol. 58, no. 5, pp. 1551–1558, 2010.
- [17] F. Costa, A. Monorchio, and G. Manara, "Efficient analysis of frequency selective surfaces by a simple equivalent circuit approach," *IEEE Antennas Propag. Mag.*, to be published.
- [18] D. M. Pozar, *Microwave Engineering*, 2nd ed. Toronto: Wiley, 1998, pp. 424–427, 162.
- [19] F. Costa and A. Monorchio, "Design of subwavelength tunable and steerable Fabry-Perot/leaky wave antennas," *Progr. Electromagn. Res.*, vol. 11, pp. 467–481, 2011.
- [20] T. K. Wu, *Frequency Selective Surface and Grid Array*. New York: Wiley, 1995.
- [21] K. N. Rozanov, "Ultimate thickness to bandwidth ratio of radar absorbers," *IEEE Trans. Antennas Propag.*, vol. 48, no. 8, pp. 1230–1234, 2000.
- [22] G. I. Kiani, K. L. Ford, K. P. Esselle, A. R. Weily, and C. J. Panagamuwa, "Oblique incidence performance of a novel frequency selective surface absorber," *IEEE Trans. Antennas Propag.*, vol. 55, no. 10, pp. 2931–2934, Oct. 2007.



Filippo Costa (S'07–M'10) was born in Pisa, Italy, on October 31, 1980. He received the M.Sc. degree in telecommunication engineering and the Ph.D. degree in applied electromagnetism in electrical and biomedical engineering, electronics, smart sensors, nano-technologies from the University of Pisa, Pisa, Italy, in 2006 and 2010, respectively.

From March to August 2009, he was a Visiting Researcher at the Department of Radio Science and Engineering, Helsinki University of Technology, TKK (now Aalto University), Finland. From January 2010

he is a Postdoctoral Researcher at the University of Pisa. His research is focused on the analysis and modelling of frequency selective surfaces and artificial impedance surfaces with emphasis to their application in electromagnetic absorbing materials, antennas, radomes, waveguide filters and techniques for retrieving dielectric permittivity of materials.



Agostino Monorchio (S'89–M'96–SM'04–F'12) received the Laurea degree in electronics engineering and the Ph.D. degree in methods and technologies for environmental monitoring from the University of Pisa, Pisa, Italy, in 1991 and 1994, respectively.

During 1995, he joined the Radio Astronomy Group, Arcetri Astrophysical Observatory, Florence, Italy, as a Postdoctoral Research Fellow, in the area of antennas and microwave systems. He has been collaborating with the Electromagnetic Communication Laboratory, Pennsylvania State University (Penn State), University Park, and he is an Affiliate of the Computational Electromagnetics and Antennas Research Laboratory. He has been a Visiting Scientist at the University of Granada, Spain, and at the Communication University of China in Beijing. He is currently an Associate Professor in the School of Engineering, University of Pisa, and Adjunct Professor at the Italian Naval Academy of Livorno. He is also an Adjunct Professor in the Department of Electrical Engineering, Penn State. He is on the Teaching Board of the Ph.D. course in "Remote Sensing" and on the council of the Ph.D. School of Engineering "Leonardo da Vinci" at the University of Pisa. His research interests include the development of novel numerical and asymptotic methods in applied electromagnetics, both in frequency and time domains, with applications to the design of antennas, microwave systems and RCS calculation, the analysis and design of frequency-selective surfaces and novel materials, and the definition of electromagnetic scattering models from complex objects and random surfaces for remote sensing applications. He has been a reviewer for many scientific journals and he has been supervising various research projects related to applied electromagnetic, commissioned and supported by national companies and public institutions.

Dr. Monorchio has served as Associate Editor of the IEEE ANTENNAS AND WIRELESS PROPAGATION LETTERS. He received a Summa Foundation Fellowship and a NATO Senior Fellowship.